Nano-optomechanics

Ewold Verhagen

Center for Nanophotonics
AMOLF
Science Park 104, 1098 XG Amsterdam, The Netherlands
verhagen@amolf.nl

1. – Introduction: coupling light and motion

The field of *optomechanics* studies the interaction between light — or, more broadly, electromagnetic fields — and the mechanical motion of objects. This interaction, mediated by optical radiation pressure forces, occurs naturally in systems where a mechanical deformation alters the optical response of the system. The mechanical motion that is considered is typically that of high-quality mechanical resonators. Such devices find application in various contexts, due to their high spectral purity and susceptibility to tiny disturbances: in atomic force microscopes, gravitational wave detectors, timekeeping (e.g. quartz oscillators in wrist watches) and signal processing (e.g. filtering high-frequency electronic signals in modern cell phones).

Light provides excellent means to read out the motion of a mechanical resonator, due to the wide abundance of high-quality laser sources and photodetectors, and because it is a probe that introduces no more extra noise than fundamental quantum (shot) noise, even at room temperature. Optical detection of motion can happen in various ways: For example, by monitoring the phase of light reflected from a mirror that is free to move, or that of light passing through an optical fiber whose refractive index is locally changed due to strain associated with a deformation of the fiber.

Indeed, a plethora of systems has been developed in recent years in which optomechanical coupling is exploited, ranging from single nanoscale beads trapped in focused laser fields, through on-chip integrated devices, all the way to the km-scale interferom-

eters that are used to detect gravitational waves. The scientific drive to develop those systems not only lies in advancing mechanical sensing performance, but in particular also in the possibilities offered by optical forces. These principles allow new ways to control mechanical systems with light, e.g. to create special quantum states of motion. Optomechanical systems thus provide a test bed for quantum physics in massive mechanical systems, for example to study potential decoherence mechanisms acting on such 'macroscopic' entities. The developed control methods allow adding mechanical resonators to the 'quantum technology toolbox', leveraging their long lifetimes and capability to couple to a variety of other (quantum) systems. In fact, through such couplings one thus also gains new ways of optical control over other degrees of freedom *via* the mechanical resonator, including over light itself. The field of optomechanics thus studies a range of phenomena from both fundamental and technological standpoints, at the intersection of quantum optics, nano- and micro-electromechanical systems (NEMS/MEMS), and photonics. It draws inspiration from related developments for gravitational wave detection, quantum information technology, and the control of cold ions and atoms with light fields.

To maximize optomechanical interactions, systems have been continuously improved along two lines: On the one hand, minimizing optical and mechanical losses — confining photons in optical cavities and phonons in mechanical resonators for the longest possible times — effectively increases their interaction. On the other hand, co-localizing light and motion in the smallest possible systems leads to large optomechanical coupling, as mechanical displacements yield larger effects on small optical cavities, and as low mass makes mechanical resonators more susceptible to optical forces. Thus, significant attention is given to *nano-optomechanical systems* that couple photons and phonons in small, on-chip architectures. In this lecture, we will introduce the basic physical description of optomechanical interactions at a tutorial level, and highlight several directions of current research. For a much more elaborate introduction to the field, including historical context, overviews of the studied systems, and in-depth theoretical descriptions, we refer the reader to several excellent other texts, including the review on 'Cavity optomechanics' by M. Aspelmeyer, T. J. Kippenberg, and F. Marquardt [1], and the book 'Quantum optomechanics' by G. Milburn and W. Bowen [2].

1˙1. *The canonical cavity optomechanical resonator.* – Although optomechanical systems take many forms, a simple model system serves to describe many of the observed phenomena in all of them. It is depicted in Fig. 1 and comprises an optical cavity of which the length can change through the motion $x(t)$ of a mechanical resonator — in this picture formed by the mass of the end mirror, whose motion is harmonically constrained by a spring. We will briefly discuss the observable (classical) effects here, before turning to a quantum description. For now, we will consider only a single optical mode (and likewise, only a single mechanical mode). This is in many cases a valid approach, when the damping of individual modes is small enough such that their resonant responses are clearly separated in frequency, and a drive laser can be tuned to interact with effectively only one cavity mode.

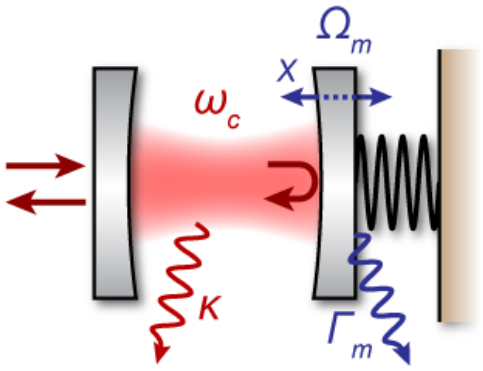

Figure 1. – A typical cavity optomechanical system, with a cavity whose optical length (and thus its frequency ω_c) is subject to the harmonic motion x of a mechanical resonator with frequency Ω_m. Optical and mechanical damping rates are κ and Γ_m, respectively.

The cavity resonance frequency $\omega_c/2\pi$ depends on the position x as

$$\omega_c(x) = \omega_c + x\partial\omega_c/\partial x + ... \tag{1}$$

We define the frequency shift per displacement as $G = -\partial\omega_c/\partial x$, which can be shown to be ω_c/L for our model system, where L is the length of the Fabry-Pérot cavity. The cavity is driven by a laser through the partially transparent left mirror. This means that light must also be able to leak out of the cavity. The rate at which energy is lost from the cavity is $\kappa/2\pi$; it is equal to the spectral linewidth of the cavity's response. The mechanical oscillator has resonance frequency $\Omega_m/2\pi$, typically in the Hz to GHz range, and in any case much smaller than $\omega_c/2\pi$. The damping rate (linewidth) of the mechanical oscillator is $\Gamma_m/2\pi$. Several effects can be discerned:

- When the frequency of a laser impinging on the cavity is tuned across its resonance, the phase of the reflected light changes by 2π over a bandwidth of $\sim \kappa$. On resonance, this extra phase shift is π (as compared to an off-resonant laser). If the mechanical oscillator moves, the resulting change of the resonance frequency is imprinted as a phase change on the reflected light of monochromatic laser of fixed frequency. The reflected phase is thus directly proportional to mirror displacement, and small motion can be read out with quantum-limited sensitivity, e.g. using homodyne interferometry.

- The light in the cavity exerts a radiation pressure force on the mechanical oscillator, which displaces it slightly in proportion to the laser power. But this changes the cavity length, and thus the cavity's optical response. As such, the optomechanical interaction can be seen as an effective optical (χ_3) nonlinearity. Moreover, as the force strongly depends on the oscillator position (for some given laser frequency),

it effectively alters the restoring force that the mechanical oscillator feels, leading to 'softening' or 'stiffening' and an associated change of the mechanical resonance frequency (the 'optical spring' effect).

- If the laser is slightly detuned from the cavity resonance, a mechanical position change will lead to a change of the light intensity in the cavity. But because of the finite response time of the cavity (given by $1/\kappa$) this change will not be instantaneous. As a result, the force on the oscillator will change — with some delay — upon a change of oscillator position. Depending on the conditions, this can lead to 'automatic' *damping* or *amplification* of the oscillator's motion. These effects, summarized under the term *dynamical backaction*, are especially pronounced in systems with small optical damping κ and small mechanical damping $\Gamma_{\rm m}$. They are at the basis of optical cooling of the mechanical resonator, for example.

In the following, we will first discuss how quantum mechanics limits the accuracy with which the mechanical motion can be measured. We will then introduce a quantum optical description of the system, and use it to describe radiation pressure effects. We will in particular discuss optical cooling and state transfer. We conclude with reviewing several research activities that exploit multimode optomechanical systems and nonlinearities to develop new ways to control light and motion in the classical and quantum domains.

2. – Quantum measurements of motion with light

2˙1. *Measuring motion with a cavity.* – The position of the mirror in Fig. 1 determines the cavity frequency, and through that the phase of an intracavity field. This, in turn, can be detected by monitoring the light leaking out of the cavity. For a laser tuned to resonance, a small displacement δx imparts a phase shift

$$\delta\phi = 4\frac{G}{\kappa}\delta x \tag{2}$$

on the outgoing laser beam. One can see the effect of cavity enhancement by comparing this shift to the $4\pi\delta x/\lambda$ phase shift that a light beam acquires by direct reflection off of a single mirror: For the Fabry-Pérot cavity, the phase shift per unit displacement is enhanced by a factor $2c/L\kappa$, which is equal to the cavity *Finesse* (the number of roundtrips light can make in the cavity before it decays) multiplied by a factor $2/\pi$.

2˙2. *Mechanical frequency response.* – So what is the motion that one typically wants to detect? A mechanical resonator is of course most likely to oscillate with a frequency near its natural resonance frequency. There, its susceptibility to external forces is highest. This susceptibility $\chi(\omega)$ specifies the displacement $x = \Re\{\tilde{x}\}$ induced by a harmonic force $\Re\{\tilde{F}_0 e^{-i\omega t}\}$ with frequency ω and (complex) amplitude $\tilde{F}_0$ through

$$\tilde{x}(t) = \tilde{x}_0 e^{-i\omega t} = \chi(\omega)\tilde{F}_0 e^{-i\omega t}. \tag{3}$$

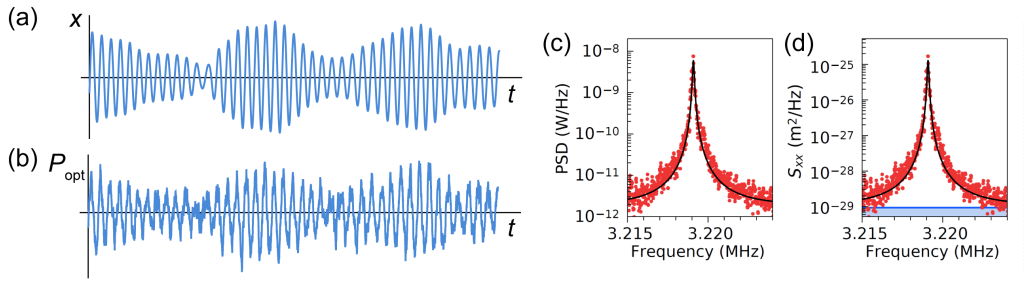

Figure 2. – (a) The amplitude and phase of the mechanical resonator's oscillations are fluctuating at a typical time scale $1/\Gamma_{\rm m}$ due to Brownian motion and quantum fluctuations. (b) A measurement of $x(t)$ through detecting optical power fluctuations $P_{\rm opt}$ will add imprecision noise. (c) Fourier-transforming the measured fluctuations using an electronic spectrum analyzer to show the electronic power spectral density (PSD) reveals the Lorentzian mechanical resonance with linewidth $\Gamma_{\rm m}$. (d) With the equipartition theorem, the spectrum can be calibrated to yield the displacement spectral density S_{xx}. The constant background (blue) is the measurement imprecision.

Note that we have introduced complex representations $\tilde{x}$ and $\tilde{F}$ of position and force, respectively, for mathematical convenience. The susceptibility is that of a damped harmonic oscillator and reads

$$\chi(\omega) = \frac{1}{m}\frac{1}{\Omega_{\rm m}^2 - \omega^2 - {\rm i}\Gamma_{\rm m}\omega}, \tag{4}$$

where m is the mass of the mechanical resonator. Near resonance of a high-Q resonator, it can be approximated as a Lorentzian response:

$$\chi(\omega) \approx \frac{\rm i}{2m\Omega_{\rm m}}\frac{1}{-{\rm i}\,(\omega - \Omega_{\rm m}) + \Gamma_{\rm m}/2}. \tag{5}$$

2˙3. *Mechanical fluctuation spectra and sidebands.* – This sharply-peaked susceptibility thus also determines the spectrum of *fluctuations* that the resonator exhibits when it is driven by a stochastic force that itself has a relatively flat spectrum. These can be both vacuum fluctuations, giving rise to zero-point motion, or thermal noise leaking into the resonator from its environment at elevated temperatures, giving rise to Brownian motion. The fluctuations are spread over a bandwidth $\sim \Gamma_{\rm m}$ around the mechanical frequency. It causes the mechanical resonator's amplitude and phase to vary randomly within a typical time scale $1/\Gamma_{\rm m}$ (see example in Fig. 2(a)). By measuring the phase fluctuations of the optical output field, one gains a record of the mechanical fluctuations $x(t)$. The fluctuation spectrum can then be obtained through a Fourier transform. We

define a 'gated' Fourier transform for a single record of measurement duration τ as [3]

$$x_\tau(\omega) = \frac{1}{\sqrt{\tau}} \int_{-\tau/2}^{\tau/2} \mathrm{d}t e^{\mathrm{i}\omega t} x(t). \tag{6}$$

Averaging many such measurements yields a smooth noise power spectrum $\langle |x_\tau(\omega)|^2 \rangle$, which approximates the *noise spectral density* $S_{xx}(\omega)$ as

$$\lim_{\tau\to\infty} \langle |x_\tau(\omega)|^2 \rangle = S_{xx}(\omega). \tag{7}$$

This is the so-called Wiener-Khinchin theorem, which relates measurable noise spectra to the Fourier transform of the autocorrelation function of $x(t)$, which is the formal definition of $S_{xx}(\omega)$[3].

The total size of the fluctuations is determined by the equipartition theorem, i.e. $m\Omega_\mathrm{m}^2\langle x^2\rangle/2 = k_B T/2$ in the limit of large temperature T, where k_B is the Boltzmann constant. For negligible temperature, only vacuum fluctuations remain, with $\langle x^2\rangle = x_\mathrm{zpf}^2$ and

$$x_\mathrm{zpf} = \sqrt{\frac{\hbar}{2m\Omega_\mathrm{m}}}. \tag{8}$$

When one measures these fluctuations at frequency Ω_m, for example using an electronic spectrum analyser that analyses the detected photocurrent of a detector in the output of an interferometer (see Fig. 2(c)), one is essentially probing the beat of an optical field at the input laser frequency ω_l and that of *optical sidebands* at frequencies $\omega_\mathrm{l} \pm \Omega_\mathrm{m}$. The fact that the mechanical motion induces such optical sidebands is entirely equivalent to Stokes and anti-Stokes Raman scattering, which produces down- or upconverted photons by giving off or taking up a quantum of energy (phonon) from a mechanical resonator. This notion is very useful, for example to distinguish quantum from classical (thermal) fluctuations: If a mechanical resonator is in its ground state, it is incapable of providing energy to upconvert a photon to higher energy. Thus, the fluctuation spectrum is necessarily asymmetric. This asymmetry can be shown to be a direct consequence of the commutation relations and can be observed e.g. by distinguishing Stokes and anti-Stokes photons through judicious spectral filtering. Indeed, such tests of *sideband asymmetry* are now standard ways to determine that a resonator has been prepared in its ground state[4].

2˙4. *Imprecision and backaction; the Standard Quantum Limit.* – What is the smallest motion that can be resolved? In order to evaluate sensitivity, we need to consider the *noise added by the measurement.* A practical measurement of $x(t)$ suffers from noise, such that a recorded trace looks more like Fig. 2(b). As a result, the observed noise spectral densities are larger than the actual fluctuations in absence of a measurement. Even if one works hard to remove all sources of technical noise, one is left with unavoidable quantum uncertainty, related to the fact that (1) the probe — light in this case — suffers from

quantum uncertainty, and (2) measurements tend to act back on the object under study. Here we will qualitatively discuss these two factors and show how they are related.

On the one hand, the shot noise of the light carrying the measured signal to the detector will produce fluctuations of the detected photocurrent. This produces a white (frequency-independent) noise 'background' in the spectra of $S_{xx}(\omega)$ that we derive from the measurement, which is called the *measurement imprecision* (fig. 2(d)). Since the amount of shot noise (as apparent on the photocurrent spectral density) scales linearly with the light intensity and the signal we seek to detect quadratically, the measurement imprecision (expressed as apparent displacement fluctuations $S_{xx}(\omega)$) reduces when we increase the laser power. In other words, we can detect phase fluctuations more accurately if we use a larger number of photons; a direct consequence of the number-phase uncertainty relationship.

However, this reduction of the measurement imprecision with increasing laser power does not come without a price. For large enough power, the shot noise of the light in the cavity starts to significantly affect the mechanical oscillator by exerting a stochastic radiation pressure force. This *measurement backaction* causes extra mechanical fluctuations $S_{xx}^{\mathrm{ba}}(\omega) = |\chi_{\mathrm{m}}(\omega)|^2 S_{FF}^{\mathrm{ba}}(\omega)$, where $S_{FF}^{\mathrm{ba}}(\omega)$ is the spectral density of the radiation pressure force fluctuations. If the cavity lifetime is shorter than the mechanical period, $S_{FF}^{\mathrm{ba}}(\omega)$ can be considered to be white noise (flat spectrum), as it originates in delta-correlated shot noise. It scales linearly with optical power, *increasing* fluctuations of the mechanical resonator even if the imprecision goes down. The total noise added by the measurement, $S_{xx}^{\mathrm{add}} = S_{xx}^{\mathrm{imp}} + S_{xx}^{\mathrm{ba}}$, evaluated at the resonance frequency of the mechanical oscillator, has a minimum for a certain optical power. This is called the *Standard Quantum Limit* (SQL). Figure 3 shows the different contributions to the noise spectra for varying probe power. It can be shown that the minimum noise is precisely equal to the spectral density of the zero-point fluctuations,

$$\bar{S}_{xx}^{\mathrm{add}}(\Omega_{\mathrm{m}}) \leq \bar{S}_{xx}^{\mathrm{zpf}}(\Omega_{\mathrm{m}}) = 2\frac{x_{\mathrm{zpf}}^2}{\Gamma_{\mathrm{m}}} = \frac{\hbar}{m\Omega_{\mathrm{m}}\Gamma_{\mathrm{m}}}. \tag{9}$$

Here, the horizontal bars denote that we are comparing 'symmetrized' spectral densities, averaged over positive and negative frequencies:

$$\bar{S}_{xx}(\omega) \equiv \left(S_{xx}(\omega) + S_{xx}(-\omega)\right)/2. \tag{10}$$

The appearance of the SQL is directly related to Heisenberg's uncertainty principle. As we are continuously monitoring the trajectory $x(t)$ in time, we gain knowledge about the oscillator's position *and* momentum. The uncertainty principle of course forbids to do this with arbitrary accuracy on both degrees of freedom. However, several clever measurement schemes exist to reduce the noise on the measurement of one of the quadratures of motion (so-called 'back-action evading' measurements) [5, 6, 7]. These include the possibility to take pulsed, 'snap-shot' measurements of displacement — which naturally gain no information on momentum — and also provide routes to creating

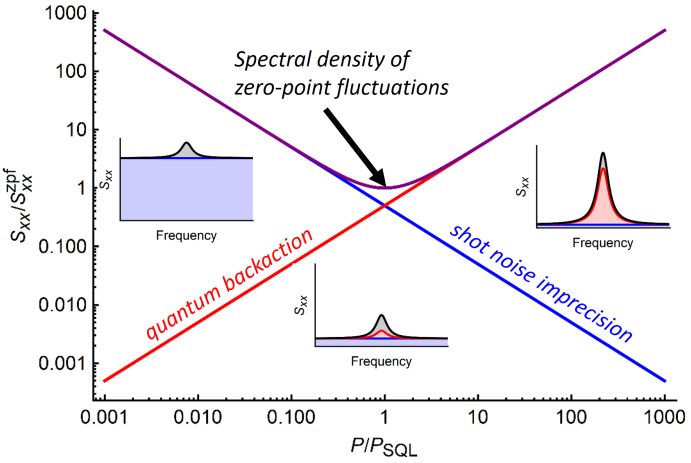

Figure 3. – Total displacement noise added by a measurement (purple) as a function of laser power. It is a combination of imprecision (blue) and backaction (red). Insets depict the measured spectra in three power regimes, when measuring zero-point fluctuations (grey).

squeezed states of the mechanical resonator, which exhibit reduced fluctuations in one of its quadratures [8, 9, 10]. Moreover, squeezed light can be used to shift the SQL to a different power for a chosen range of frequencies. Such methods are crucial to the working of the next generation gravitational wave detectors, which will operate at conditions close to the quantum limit [11].

We note that many optomechanical systems can now operate at measurement strengths way beyond the standard quantum limit power $P_{\rm SQL}$. That does not automatically mean that radiation-pressure-induced fluctuations dominate the resonator's motion: After all, since for most systems $k_B T \gg \hbar\Omega_{\rm m}$, thermal fluctuations typically dwarf quantum motion. However, several optomechanical experiments achieved the regime where quantum backaction induces fluctuations of comparable size to thermal motion [12, 13, 14].

3. – A quantum optical description of cavity optomechanics

3˙1. *The optomechanical Hamiltonian.* – In the preceding section, we already recognized the (back)action of optical forces in optomechanical systems. The interactions mediated by these forces lead to rich behaviour. To introduce this, we will now discuss the basic cavity optomechanical system in terms of the annihilation operators $\hat{a}$ and $\hat{b}$ of the optical cavity and mechanical resonator modes, respectively. The Hamiltonian of the combined oscillators can be written as

$$\hat{H} = \hbar\omega_{\rm c}(\hat{x})\hat{a}^\dagger\hat{a} + \hbar\Omega_{\rm m}\hat{b}^\dagger\hat{b} = \hbar\omega_{\rm c}\hat{a}^\dagger\hat{a} + \hbar\Omega_{\rm m}\hat{b}^\dagger\hat{b} - \hbar G\hat{x}\hat{a}^\dagger\hat{a}, \tag{11}$$

where we recognized that the optical frequency depends linearly on the position $\hat{x}$ as $\omega_{\rm c}(\hat{x}) = \omega_{\rm c} - G\hat{x}$. We choose the origin of x such that the mean position $\bar{x} = \langle\hat{x}\rangle = 0$. From the interaction term on the right, we immediately recognize the radiation pressure force

$$F_{\rm rp} = \hbar G\hat{a}^\dagger\hat{a}. \tag{12}$$

Since $\hat{x}$ can be expressed in terms of the phonon ladder operators as $\hat{x} = x_{\rm zpf}(\hat{b} + \hat{b}^\dagger)$, we can write the cavity optomechanical Hamiltonian as

$$\hat{H} = \hbar\omega_{\rm c}\hat{a}^\dagger\hat{a} + \hbar\Omega_{\rm m}\hat{b}^\dagger\hat{b} - \hbar g_0\hat{a}^\dagger\hat{a}(\hat{b} + \hat{b}^\dagger), \tag{13}$$

where we have introduced the *vacuum optomechanical coupling rate* $g_0 = Gx_{\rm zpf}$. This parameter signifies the optical frequency shift for a displacement by the size of the quantum ground state, and is a general measure of photon-phonon coupling strength, ignorant of e.g. the arbitrariness in defining x. Significant advances have been made towards optimizing this parameter, especially in nanoscale devices. In electromechanical systems, mechanical motion is coupled to the GHz-frequency electromagnetic modes of on-chip superconducting LC-resonators. Especially large coupling strengths are obtained by letting the motion of thin micron-scale aluminum drums affect the capacitance across a gap of few tens of nm [15]. Largest coupling strength are achieved in nanophotonic systems, such as high-index ring resonators where light is coupled to breathing motion of the ring [16], and especially photonic crystal cavities [17, 18, 19, 20, 21]. There, light trapped in nanobeam cavities within wavelength-scale mode volumes interacts with localized mechanical vibrations, either flexural beam vibrations at MHz frequencies or breathing motion of the beam at GHz frequencies. In such systems, coupling rates $g_0/2\pi$ up to a few tens of MHz have been achieved [22]. Optomechanical shifts are optimized through design, and originate in the movement of dielectric boundaries near large field concentrations (akin to an optical gradient force) [23] or in strain-induced changes of the refractive index (electrostriction) [24].

3˙2. *The linearized Hamiltonian.* – Interestingly, the interaction term in Hamiltonian 13 is cleary nonlinear; it contains products of more than two operators. This in principle can lead to very interesting quantum behaviour, including the generation of nonclassical states of motion and light and single-quantum interactions [25, 26]. This nonlinearity can be seen, for example, in a simple thought experiment: A photon entering the cavity on resonance exerts a force, displacing the resonator. This, in turn, shifts the cavity frequency such that a second photon of the same frequency can no longer enter the cavity, establishing a form of single-photon blockade. However, for any such effect to be observable, the cavity linewidth — which the Hamiltonian ignored — should be smaller than the mechanical frequency and the photon-phonon coupling rate; $g_0 > \Omega_{\rm m} > \kappa$. This is so far out of reach for solid-state optomechanical systems, by about two orders of magnitude.

While it is conceivable that the single-quantum nonlinear regime of optomechanics is reached in the future, a great degree of quantum control is still achievable for interaction strengths reachable today, by enhancing the interaction through suitable laser drive fields [1, 2]. To see how this comes about, we first transform the Hamiltonian 13 to a frame rotating at the laser frequency ω_l. A transformation is performed through a unitary operator $\hat{U}$, which changes the Hamiltonian $\hat{H}$ as

$$\hat{H} \to \hat{U}\hat{H}\hat{U}^\dagger - \hat{U}\mathrm{i}\hbar\partial\hat{U}^\dagger/\partial t. \tag{14}$$

To shift to a rotating frame, we take $\hat{U} = \exp\left(\mathrm{i}\omega_\mathrm{l}\hat{a}^\dagger\hat{a}t\right)$ ([1]), to arrive at

$$\hat{H} = -\hbar\Delta\hat{a}^\dagger\hat{a} + \hbar\Omega_\mathrm{m}\hat{b}^\dagger\hat{b} - \hbar g_0\hat{a}^\dagger\hat{a}(\hat{b} + \hat{b}^\dagger), \tag{15}$$

where we introduced the *laser detuning* $\Delta \equiv \omega_\mathrm{l} - \omega_\mathrm{c}$. We note that in the Heisenberg picture, this Hamiltonian now describes the evolution of slowly varying operators $\hat{a}$ (analogous to the light field in the cavity), etc.

We now consider that the cavity is driven by a coherent laser to large amplitude. It then makes sense to write $\hat{a} = \alpha + \delta\hat{a}$, where $\alpha \equiv \langle\hat{a}\rangle = \sqrt{\bar{n}_c}$ is the (complex) amplitude of the light field in the cavity expressed as the square root of the mean number of photons $\bar{n}_c$, and all fluctuations of the optical field are contained in $\delta\hat{a}$. Thus, when expanding the photon number, we get

$$\hat{a}^\dagger\hat{a} = |\alpha|^2 + \alpha^*\delta\hat{a} + \alpha\delta\hat{a}^\dagger + \delta\hat{a}^\dagger\delta\hat{a}. \tag{16}$$

We now insert this in eq. 15 and neglect all terms with $\delta\hat{a}^\dagger\delta\hat{a}$ assuming large drive $|\alpha| \gg 1$. The interaction part of the Hamiltonian (last term in eq. 15) then reads

$$\hat{H}_\mathrm{int} \approx -\hbar g_0|\alpha|^2(\hat{b} + \hat{b}^\dagger) - \hbar g_0(\alpha^*\delta\hat{a} + \alpha\delta\hat{a}^\dagger)(\hat{b} + \hat{b}^\dagger). \tag{17}$$

The first term corresponds to a constant shift of the mechanical displacement due to the radiation pressure of the classical drive field. We can omit it by implementing an appropriate shift of the displacement's origin and then in the following always use a new detuning with respect to the (shifted) cavity resonance $\Delta \to \Delta - 2g_0^2|\alpha|^2/\Omega_\mathrm{m}$. Moreover, for a single optical mode we can always choose an appropriate gauge of intracavity phase such that α is real. The interaction then becomes

$$\hat{H}_\mathrm{int} \approx -\hbar g(\delta\hat{a} + \delta\hat{a}^\dagger)(\hat{b} + \hat{b}^\dagger). \tag{18}$$

Here we have introduced the *linearized coupling rate* $g = g_0\alpha$. This Hamiltonian describes two *linearly coupled harmonic oscillators* at resonance frequencies $-\Delta$ and Ω_m, coupled at a rate g that is controllable with the external laser drive. Note that the

---

([1]) For this transformation, $\hat{U}\hat{a}\hat{U}^\dagger = e^{-\mathrm{i}\omega_\mathrm{l}t}\hat{a}$, $\hat{U}\hat{a}^\dagger\hat{U}^\dagger = e^{\mathrm{i}\omega_\mathrm{l}t}\hat{a}^\dagger$, and $\hat{U}\mathrm{i}\hbar\partial\hat{U}^\dagger/\partial t = \hbar\omega_\mathrm{l}\hat{a}^\dagger\hat{a}$.

optical cavity mode $\delta\hat{a}$ is the displaced field, describing the *fluctuations* of the light field, i.e. the photons in sidebands of the drive field α. All dynamics of the system can be deduced from the full Hamiltonian, by retrieving the evolution of an operator $\hat{A}$ in the Heisenberg picture through $\dot{\hat{A}} = \frac{\mathrm{i}}{\hbar}[\hat{H}, \hat{A}]$ [1].

This interaction Hamiltonian describes many phenomena in optomechanics: it shows how mechanical position fluctuations $(\hat{b}+\hat{b}^\dagger)$ are transduced to the optical phase quadrature $(\delta\hat{a} + \delta\hat{a}^\dagger)$ to facilitate motion measurement. And just like in classical coupled oscillators, or atom-light coupling in cavity QED, we can distinguish weak and strong coupling regimes when $2g < \{\kappa, \Gamma_\mathrm{m}\}$ and $2g > \{\kappa, \Gamma_\mathrm{m}\}$, respectively. In the strong coupling regime, fluctuation spectra display normal mode splitting and Rabi oscillations between photons and phonons occur [27, 28, 15, 29]. In the weak coupling regime, the optical cavity (plus the bath it decays to) can be considered to influence the decay rate of the mechanical resonator in processes analogous to the Purcell effect in cavity QED. This is in fact the source of optical cooling and amplification, effects known as dynamical backaction [1, 30, 31].

4. – Optomechanical cooling and state transfer

4˙1. *The resolved sideband regime.* – If the optical (and mechanical) damping is smaller than the mechanical frequency, the two oscillators are only coupled efficiently when they are tuned to resonance, i.e. for $\Delta \approx \pm\Omega_\mathrm{m}$. To see what effect this has, we first shift to an interaction picture by applying a new unitary (rotating frame) transformation

$$\hat{U} = e^{-\mathrm{i}\Delta\delta\hat{a}^\dagger\delta\hat{a}t + \mathrm{i}\Omega_\mathrm{m}\hat{b}^\dagger\hat{b}t}, \tag{19}$$

such that the Hamiltonian becomes

$$\hat{H}_\mathrm{int} = -\hbar g\left(\delta\hat{a}\hat{b}^\dagger e^{\mathrm{i}(\Delta+\Omega_\mathrm{m})t} + \delta\hat{a}^\dagger\hat{b}e^{-\mathrm{i}(\Delta+\Omega_\mathrm{m})t} + \delta\hat{a}\hat{b}e^{\mathrm{i}(\Delta-\Omega_\mathrm{m})t} + \delta\hat{a}^\dagger\hat{b}^\dagger e^{-\mathrm{i}(\Delta-\Omega_\mathrm{m})t}\right) \tag{20}$$

Provided that $(\kappa, \Gamma_\mathrm{m}) < \Omega_\mathrm{m}$, the so-called *resolved sideband regime*, and likewise $g < \Omega_\mathrm{m}$, we can apply the *rotating wave transformation* to neglect some terms in the above Hamiltonian. In particular, if the laser is detuned to the red mechanical sideband of the cavity ($\Delta = -\Omega_\mathrm{m}$), we can neglect the last two terms in the interaction Hamiltonian on the basis that they are oscillating very fast (at $\pm 2\Omega_\mathrm{m}$) compared to the slowly varying (resonant) first two terms and the cavity dynamics. For that detuning,

$$\hat{H}_\mathrm{int} = -\hbar g(\delta\hat{a}^\dagger\hat{b} + \delta\hat{a}\hat{b}^\dagger). \tag{21}$$

The evolution that this 'beam-splitter' Hamiltonian describes corresponds to a continuous swapping of the states between the optical and mechanical degrees of freedom at a rate $2g$. It thus enables *state transfer* between the optical and mechanical modes. For a coherent drive, the optical field $\delta\hat{a}$ corresponds to the vacuum, such that transfer of this

state to the mechanical mode naturally cools it. This is the principle of *resolved sideband cooling* [32, 33].

For blue detuning ($\Delta = \Omega_{\rm m}$), a similar argument selects the last two terms:

$$\hat{H}_{\rm int} = -\hbar g(\delta\hat{a}^\dagger\hat{b}^\dagger + \delta\hat{a}\hat{b}). \tag{22}$$

With this 'two-mode squeezing' Hamiltonian, the simultaneous creation of a photon and a photon can lead to entanglement between the light field and the mechanical motion, as well as the aforementioned amplification and self-oscillations.

4˙2. *Cooling rate and engineered reservoir.* – Particular attention has been given to optomechanical cooling, as it provides a way to prepare macroscopic resonators, which normally suffer from significant thermal fluctuations, to their quantum ground state [32, 33]. Laser cooling happens most effectively in the weak coupling regime at detuning $\Delta = -\Omega_{\rm m}$, where the state transfer Hamiltonian 21 applies. Without cooling, a mechanical resonator in equilibrium with a bath at temperature T, to which it is coupled with rate $\Gamma_{\rm m}$, is typically in a large thermal state with mean phonon occupation $\bar{n}_{\rm th} = k_{\rm B}T/\hbar\Omega_{\rm m}$. The cooling process can be pictured hand-wavingly as follows: under the influence of the interaction, the displaced optical field $\delta\hat{a}$ is swapped to the mechanical resonator, bringing it to its ground state. In turn, the thermal phonons are swapped to the optical mode, from which they rapidly dissipate in the cold bath that the optical mode is coupled to with decay rate κ. Thus, the optical cavity provides a path of decay for the mechanical resonator, in addition to the intrinsic mechanical decay $\Gamma_{\rm m}$ (see Fig. 4). It introduces a reservoir to the mechanical resonator that is intrinsically cold. The rate of decay via the cavity is

$$\Gamma_{\rm opt} = \frac{4g^2}{\kappa}. \tag{23}$$

Provided that the total mechanical damping rate $\Gamma_{\rm eff} = \Gamma_{\rm opt} + \Gamma_{\rm m}$ remains smaller than the cavity decay rate κ, the cooling rate can be increased by ramping up the laser intensity. When the red-detuned cooling laser is applied, the total damping rate of the resonator changes to $\Gamma_{\rm eff} = \Gamma_{\rm opt} + \Gamma_{\rm m}$, and the fluctuations are reduced. In a classical theory, the effective temperature of the mechanical mode could go to zero, according to $T_{\rm eff} = T\Gamma_{\rm m}/\Gamma_{\rm eff}$. This is however only true for narrow-linewidth cavities, such that Stokes processes, described by the interaction terms in eq. 22, are suppressed. If not, these interactions — which are essentially the aforementioned quantum backaction — add more phonons to the resonator than can be cooled. It can be shown that the minimum achievable phonon number (in the limit of large laser power) is $\bar{n}_{\rm min} = (\kappa/4\Omega_{\rm m})^2$ [32, 33].

In conclusion, in the resolved sideband regime the phonon number can become smaller than 1 and the system can be cooled close to the mechanical ground state. This has been achieved in 2011 for the first time at NIST in a nanoscale electromechanical system, and since then reached in various other systems [34, 35, 36].

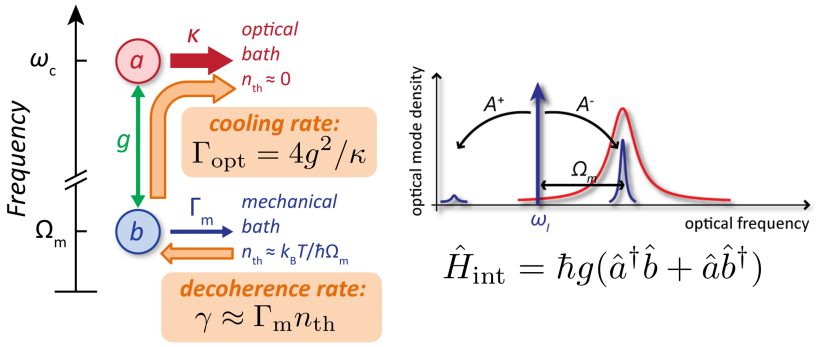

Figure 4. – (left) Schematic of optical cooling as a competition between different environments. The mechanical resonator 'b' is coupled at rate g to an optical mode a. Decay to the optical bath thus competes with the intrinsic mechanical bath, characterized by a much larger thermal occupancy $n_{\rm th}$. Thus, thermomechanical fluctuations entering the mechanical mode at rate γ can be quickly dissipated in the optical bath, which is carrying no more than quantum fluctuations, leading to a net cooling of the mechanical oscillator. (right) The cooling can be seen as a cavity enhancement of anti-Stokes scattering processes A^-. In the resolved sideband regime $\Omega_{\rm m} > \kappa$ the Stokes scattering A^+ is sufficiently suppressed to not imprint excess backaction fluctuations.

5. – Controlling photons and phonons

The above dynamics reveal a glimpse into the effects that are studied in optomechanics research which is by no means exhaustive. The interactions in these relatively simple systems have sparked a wide variety of pursuits towards controlling both photons and phonons in new ways, in both quantum and classical contexts. The latter includes applications within time-keeping and signal synthesis and processing that exploit the generation of narrow-band mechanical oscillations. Indeed, in the standard optomechanical system a blue-detuned laser drive induces mechanical amplification through dynamical backaction, i.e., enhancement of the Stokes scattering process. For high enough optical power, this negative $\Gamma_{\rm opt}$ overcomes intrinsic dissipation, resulting in a net mechanical gain. Laser powers above this parametric instability threshold thus drive the mechanical resonator into a regime of large self-oscillations reminiscent of lasing behaviour. The amplitude of these oscillations is limited through nonlinear effects.

5˙1. *Optomechanically-induced transparency and cooperativity*. – Moreover, the coupling between optical and mechanical modes, induced by a detuned drive laser, also provides a way to control the propagation of optical signals. An example is the effect of optomechanically-induced transparency (OMIT): If a cavity is critically coupled to an input/output channel, an optical 'probe' laser field tuned to cavity resonance $\omega_{\rm c}$ is normally absorbed. But in the presence of a red-detuned drive at $\omega_{\rm c} - \Omega_{\rm m}$, the beat of drive and probe can resonantly induce mechanical vibrations. These in turn stimulate the creation of a modulation sideband of the drive laser at $\omega_{\rm c}$ — which can destructively

interfere with the probe field in the cavity. The result is a narrow frequency window of finite optical transparency. In essence, the two-way optomechanical coupling described by eq. 21 provides an extra path photon-phonon-photon that excitations can take in the system, and that can interfere with other paths. Similar effects of optomechanically-induced absorption and amplification arise in the red-detuned regime due to the interaction in eq. 22.

The OMIT window can be controlled by the drive laser, and leads to near-ideal transmission at high drive power. The transparency becomes significant (exceeding 1/4) if the so-called optomechanical *cooperativity* C exceeds unity. The cooperativity is defined as

$$C = \frac{4g^2}{\kappa\Gamma_{\rm m}}. \tag{24}$$

This quantity, which combines coupling strength and dissipation, describes the strength of many other optomechanical effects as well. For example, the condition $C = 1$ also defines the optical field strength at which the standard quantum limit is reached.

A related quantity of importance is the *quantum cooperativity* $C_q = C/\bar{n}_{\rm th}$, which is effectively the cooperativity with mechanical dissipation rate replaced by thermal decoherence rate $\gamma = \Gamma_{\rm m}\bar{n}_{\rm th}$. Reaching $C_q > 1$ is a general condition for achieving optomechanical control in the quantum regime: It enables laser cooling to thermal occupancies below 1 (either through sideband or active feedback cooling) [34, 35, 14], the observation of radiation pressure shot noise at equal level as thermal fluctuations [12], effects such as optical and mechanical quantum squeezing [37, 38], quantum-coherent transfer of signals [29, 39], etc.

5˙2. *Beyond single-mode interactions.* – A wide array of possibilities emerges when extending optomechanical systems beyond the single optical and single mechanical modes that compose the model system we discussed so far. For example, if two mechanical modes are both coupled to a single optical cavity mode, as depicted in Fig. 5(a), a laser field can lead to mechanical coupling: If the laser is detuned from cavity resonance, the motion of one resonator will lead to a change of the intracavity photon number and thus a change of the force on the other resonator, and vice versa. The condition for strong mechanical coupling is $C > 1$ [40], and if the coupling exceeds decoherence (for $C_q > 1$), the light field entangles the mechanical resonators [41]. Moreover, when combined with self-oscillation and mechanical amplification, such systems allow the control and study of synchronization of (nano)mechanical oscillators [42, 43, 44].

Conversely, if two optical modes are coupled to a single mechanical mode, as depicted in Fig. 5(b), optical control fields can stimulate coupling of the two optical modes *via* the mechanical resonator. The state-transfer Hamiltonian 21 can be straightforwardly extended to two optical modes if they are both excited by suitably red-detuned drive fields. For large — and matched — cooperativities, probe light entering one cavity on resonance will exit via the other. This mode conversion process preserves quantum coherence if $C_q > 1$ [45, 46, 47].

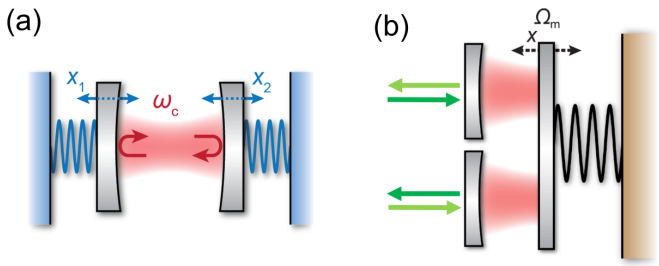

Figure 5. – Examples of multimode optomechanical systems. (a) Two mechanical resonators can be coupled via radiation pressure of a single cavity mode. (b) Two optical resonators interacting with a single mechanical resonator facilitate state transfer from one cavity to the other via the mechanical resonator.

Interestingly, the two cavity modes do not need to be at equal frequency, as long as they are driven with suitable drive fields that create the couplings (Fig. 6(a)). In fact, the parametric optomechanical coupling even allows state transfer from microwave to optical signals [48]. This provides a promising technological opportunity, as such a quantum-coherent link would be a nice way to connect optical photons — which can transport quantum information virtually decoherence free at room temperature — to quantum computers based on superconducting circuits that operate at GHz frequencies. Multiple groups are thus pursuing the creation of such interfaces, by suitably combining optical and microwave cavities with nanomechanical resonators [49, 50, 51, 52, 53].

5˙3. *Beyond reciprocity*. – The fact that the parametric coupling mechanisms we discussed provide conversion between optical and mechanical excitations at different frequencies offers more interesting opportunities. These relate to the notion that optomechanical interactions can effectively break time-reversal symmetry for light or sound. For

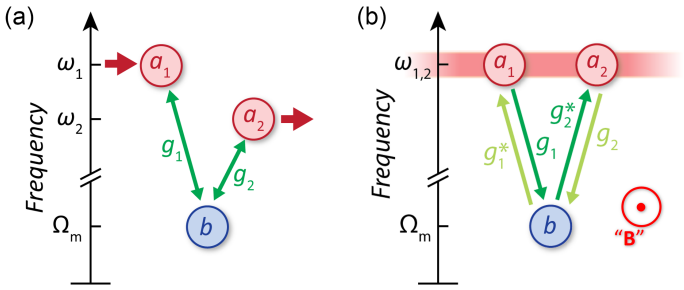

Figure 6. – Wavelength conversion and nonreciprocity using optomechanical coupling. (a) Two drive fields mediate conversion of an optical signal from one cavity mode to another, via the mechanical resonator. (b) As the phases of drive fields are imprinted on the photon-phonon transfer in a nonreciprocal fashion, mechanically-mediated mode conversion can lead to effective magnetif fields for light and sound.

charged particles such as electrons, magnetic fields can break time-reversal symmetry and induce rich physical behaviour, from cyclotron orbits that depend on propagation direction, to the Aharonov-Bohm effect which imprints a direction-dependent phase on the wavefunction of a particle traversing a loop that encloses a magnetic flux, and one-way transport in topologically protected edge states of quantum Hall insulators. These effects have in common that they break reciprocity: If source and detector are exchanged, transport amplitude and phase is not preserved.

Photons and phonons, in contrast, do not interact with magnetic fields (except very weakly in magneto-optic materials). To create on-chip nonreciprocal and topological components that break time-reversal symmetry in a similar way, optomechanical interactions in multimode systems provide an interesting toolbox. When going from eq. 17 to eq. 18, we ignored the phase of the drive field α. This was possible for a single optical mode through an appropriate change of gauge. But in multimode systems, the phase *difference* of drive fields cannot be generally gauged away, such that we should remember to describe the coupling rates g for all modes as complex quantities, with phases directly related to those of the optical drive fields. For example, for red detuned drives the interaction Hamiltonian is generally of the form $-\hbar(g\delta\hat{a}^\dagger\hat{b} + g^*\delta\hat{a}\hat{b}^\dagger)$ for each coupling. Here we see that the optical drive phase is imprinted nonreciprocally on the photon-phonon transfer: If the creation of a phonon upon annihilation of a photon gains a positive phase, the reverse path creating a photon in the same mode gains a negative phase. This is reminiscent of the Peierls phase that electron wavefunctions gain as they travel in a magnetic vector potential. So if a photon transferred from mode 1 to mode 2 via a mechanical resonator acquires a phase $\Delta\phi = \arg(g_1) - \arg(g_2)$ (where g_i defines the drive-induced coupling rate of the resonator to each mode i), the reverse process from mode 2 to 1 acquires a phase $-\Delta\phi$. In analogy to the electronic Aharonov-Bohm effect, this becomes observable when a path with such a nonreciprocal phase is interfered with a different path (see Fig. 6(b)). In suitably driven optomechanical systems, this has been used to create nonreciprocal optical and microwave elements such as isolators and circulators, by implementing constructive interference of paths from one port to another, but destructive in the opposite direction [54, 55, 56, 57, 58, 59, 60, 61, 62, 63]. Similar mechanisms can also be used to break reciprocity for optically-mediated mechanical mode transfer [64, 65].

These effects rely on optical and mechanical resonances, and are thus inherently limited in bandwidth. The bandwidths can exceed the mechanical linewidth, as often the optically damped linewidth Γ_{eff} is the relevant bandwidth over which transport can be controlled. Nonetheless, also those are typically limited fundamentally by the cavity linewidth and/or the mechanical frequency. Various schemes seek to control photon and phonon transport over larger bandwidths, by exploiting propagating light and sound waves in waveguides rather than cavities. While the absence of resonant enhancement makes cavity-less approaches challenging, promising results have been achieved [66, 67].

Extending the creation of effective magnetic fields for optical or mechanical transport to large numbers of modes in optomechanical lattices provides many opportunities. These include in particular the creation of topological insulators for light and sound [68], with

intriguing properties such as one-way conduction of signals along the edge of the array, topologically protected against backscattering. A flexible platform towards such goals is offered by periodically structured dielectric slabs: Suitable patterns can offer simultaneous two-dimensional bandgaps for both light and sound at the nanoscale, with point or line defects in the structure serving as optomechanical resonators and waveguides connecting them [69]. While the control over fabrication disorder makes the implementation of such arrays challenging, continuous technical improvements could bring it into reach in the near future.

5˙4. *Beyond linearity*. – To create non-classical states of light or motion, a certain resource of nonlinearity is needed. Although the intrinsic nonlinearity of the optomechanical Hamiltonian 13 can have pronounced effects on thermal fluctuations with $\bar{n}_{\mathrm{th}} \gg 1$ [22], the regime where this nonlinearity is significant at the single-quantum level is still out of reach for massive mechanical resonators.

Various techniques are however pursued to introduce nonlinearity in different ways. A straightforward strategy to create a Hamiltonian describing a nonlinear coupling between optical fields and motion is to enhance so-called *quadratic coupling* through design. If a system is designed such that the linear term in the relation between optical frequency and position in eq. 1 vanishes, the first leading term will likely be quadratic ($\omega_{\mathrm{c}} \propto x^2$). In the resolved sideband regime, this leads to a Hamiltonian that directly couples phonon number $\hat{b}^\dagger\hat{b}$ to the light field. This naturally occurs for example when a vibrating membrane is placed exactly in the middle of a Fabry-Pérot cavity [70]. Especially if the reflectivity of the membrane is high, the quadratic variation with position can be pronounced [71, 72]. Quadratic coupling can in principle lead to the creation of nonclassical states (e.g. resembling superpositions of x and $-x$), and to the detection of quantum jumps when single mechanical quanta enter or exit the mechanical mode [70, 73]. However, careful analysis shows that sufficient cancellation of linear coupling puts stringent demands on loss and fabrication precision that are equivalent to those to reach single-photon strong coupling $g_0 > \kappa$ [74] — although nanoscale confinement in specific electromechanical systems may somewhat relax those demands [75].

Thus, a multitude of efforts aim to couple intrinsically nonlinear quantum systems to mechanical resonators in one way or another. An interesting approach is to leverage the fact that *single-photon detectors* are inherently nonlinear [76, 77, 78] For a laser tuned to the blue sideband of an optical cavity, the detection of a single photon emitted on cavity resonance (in the Stokes sideband) 'heralds' the presence of a single phonon if the resonator was initially cooled to its ground state, as the phonon and Stokes photon must have been created as a pair through the $\hat{a}^\dagger\hat{b}^\dagger$ term in the Hamiltonian. A subsequent 'click' that detects an anti-Stokes photon for a red-detuned laser can prove the presence of that phonon — as long as it was performed within a mechanical decoherence time. Such protocols have been used for example to study entanglement between mechanical vibrations of distant photonic crystal nanobeams, and nonclassical states of motion that are conditioned on the detection of single photons [79, 80]

To introduce quantum nonlinearity in a more deterministic fashion, researchers strive

to couple mechanical resonators to two-level systems, creating mechanical analogues of cavity or circuit quantum electrodynamics — or the motion of trapped ions coupled to two-level transitions [81]. For example, it has been proposed and demonstrated that mechanical motion can influence the transition frequencies of semiconductor quantum dots and nitrogen vacancy centers [82, 83, 84, 85, 86], or coupled to the latter via a magnetic field gradient [86]. Moreover, optical emitters placed in suitable laser-driven optomechanical systems can lead to phonon-emitter interactions [87, 88]. At this moment the most advanced demonstrations have been provided using the techniques of circuit QED, coupling superconducting qubits based on Josephson junctions to high-frequency bulk or surface acoustic wave resonators through piezo-electric interactions, achieving high levels of control over the quantum motion of resonators involving billions to trillions of moving atoms [89, 90, 91, 92].

6. – Conclusions

The field of cavity optomechanics, and in particular nano-optomechanics, has proven a fertile ground to explore various intriguing physical concepts and develop technology that could impact classical and quantum information processing as well as sensing and metrology. Spectacular advances in system performance and control techniques, as well as interfacing with other (quantum) systems in hybrid architectures, continue to show the ability of optomechanics to create new scientific opportunities.

Acknowledgements. – This work is part of the research programme of the Netherlands Organisation for Scientific Research (NWO). E.V. acknowledges support from the Office of Naval Research (grant no. N00014-16-1-2466), an NWO Vidi grant, the European Research Council (ERC Starting Grant no. 759644-TOPP), and the European Union's Horizon 2020 research and innovation programme under grant agreement no. 732894 (FET Proactive HOT).

REFERENCES

[1] ASPELMEYER M., KIPPENBERG T. J. and MARQUARDT F., *Rev. Mod. Phys.*, **86** (2014) 1391.
[2] BOWEN W. P. and MILBURN G. J., *Quantum Optomechanics* (CRC Press) 2015.
[3] CLERK A. A., DEVORET M. H., GIRVIN S. M., MARQUARDT F. and SCHOELKOPF R. J., *Rev. Mod. Phys.*, **82** (2010) 1155.
[4] SAFAVI-NAEINI A. H., CHAN J., HILL J. T., ALEGRE T. P. M., KRAUSE A. and PAINTER O., *Phys. Rev. Lett.*, **108** (2012) 033602.
[5] CLERK A. A., MARQUARDT F. and JACOBS K., *New J. Phys.*, **10** (2008) 095010.
[6] HERTZBERG J. B., ROCHELEAU T., NDUKUM T., SAVVA M., CLERK A. A. and SCHWAB K. C., *Nat. Phys.*, **6** (2010) 213.
[7] SUH J., WEINSTEIN A. J., LEI C. U., WOLLMAN E. E., STEINKE S. K., MEYSTRE P., CLERK A. A. and SCHWAB K. C., *Science*, **344** (2014) 1262.
[8] VANNER M. R., PIKOVSKI I., COLE G. D., KIM M. S., BRUKNER Č., HAMMERER K., MILBURN G. J. and ASPELMEYER M., *PNAS*, (2011) .

[9] VANNER M. R., HOFER J., COLE G. D. and ASPELMEYER M., *Nat. Commun.*, **4** (2013) 2295.
[10] MUHONEN J. T., LA GALA G. R., LEIJSSEN R. and VERHAGEN E., *arXiv:1812.09720*, (2018) .
[11] AASI J. and ET AL., *Nat. Photon.*, **7** (2013) 613.
[12] PURDY T. P., PETERSON R. W. and REGAL C. A., *Science*, **339** (2013) 801.
[13] WILSON D. J., SUDHIR V., PIRO N., SCHILLING R., GHADIMI A. and KIPPENBERG T. J., *Nature*, **524** (2015) 325.
[14] ROSSI M., MASON D., CHEN J., TSATURYAN Y. and SCHLIESSER A., *Nature*, **563** (2018) 53.
[15] TEUFEL J. D., LI D., ALLMAN M. S., CICAK K., SIROIS A. J., WHITTAKER J. D. and SIMMONDS R. W., *Nature*, **471** (2011) 204.
[16] DING L., BAKER C., SENELLART P., LEMAITRE A., DUCCI S., LEO G. and FAVERO I., *Phys. Rev. Lett.*, **105** (2010) 263903.
[17] EICHENFIELD M., CAMACHO R., CHAN J., VAHALA K. J. and PAINTER O., *Nature*, **459** (2009) 550.
[18] EICHENFIELD M., CHAN J., CAMACHO R. M., VAHALA K. J. and PAINTER O., *Nature*, **462** (2009) 78.
[19] GAVARTIN E., BRAIVE R., SAGNES I., ARCIZET O., BEVERATOS A., KIPPENBERG T. J. and ROBERT-PHILIP I., *Phys. Rev. Lett.*, **106** (2011) 203902.
[20] SAFAVI-NAEINI A. H., ALEGRE T. P. M., CHAN J., EICHENFIELD M., WINGER M., LIN Q., HILL J. T., CHANG D. E. and PAINTER O., *Nature*, **472** (2011) 69.
[21] LEIJSSEN R. and VERHAGEN E., *Sci. Rep.*, **5** (2015) 15974.
[22] LEIJSSEN R., LA GALA G. R., FREISEM L., MUHONEN J. T. and VERHAGEN E., *Nat. Commun.*, **8** (2017) 16024.
[23] JOHNSON S. G., IBANESCU M., SKOROBOGATIY M. A., WEISBERG O., JOANNOPOULOS J. D. and FINK Y., *Phys. Rev. E*, **65** (2002) 066611.
[24] CHAN J., SAFAVI-NAEINI A. H., HILL J. T., MEENEHAN S. and PAINTER O., *Appl. Phys. Lett.*, **101** (2012) 081115.
[25] RABL P., *Phys. Rev. Lett.*, **107** (2011) 063601.
[26] NUNNENKAMP A., BØRKJE K. and GIRVIN S. M., *Phys. Rev. Lett.*, **107** (2011) 063602.
[27] DOBRINDT J. M., WILSON-RAE I. and KIPPENBERG T. J., *Phys. Rev. Lett.*, **101** (2008) 263602.
[28] GRÖBLACHER S., HAMMERER K., VANNER M. R. and ASPELMEYER M., *Nature*, **460** (2009) 724.
[29] VERHAGEN E., DELÉGLISE S., WEIS S., SCHLIESSER A. and KIPPENBERG T. J., *Nature*, **482** (2012) 63.
[30] KIPPENBERG T. J., ROKHSARI H., CARMON T., SCHERER A. and VAHALA K. J., *Phys. Rev. Lett.*, **95** (2005) 033901.
[31] KIPPENBERG T. J. and VAHALA K. J., *Science*, **321** (2008) 1172.
[32] WILSON-RAE I., NOOSHI N., ZWERGER W. and KIPPENBERG T. J., *Phys. Rev. Lett.*, **99** (2007) 093901.
[33] MARQUARDT F., CHEN J. P., CLERK A. A. and GIRVIN S. M., *Phys. Rev. Lett.*, **99** (2007) 093902.
[34] TEUFEL J. D., DONNER T., LI D., HARLOW J. W., ALLMAN M. S., CICAK K., SIROIS A. J., WHITTAKER J. D., LEHNERT K. W. and SIMMONDS R. W., *Nature*, **475** (2011) 359.
[35] CHAN J., ALEGRE T. P. M., SAFAVI-NAEINI A. H., HILL J. T., KRAUSE A., GRÖBLACHER S., ASPELMEYER M. and PAINTER O., *Nature*, **478** (2011) 89.

[36] PETERSON R. W., PURDY T. P., KAMPEL N. S., ANDREWS R. W., YU P.-L., LEHNERT K. W. and REGAL C. A., *Phys. Rev. Lett.*, **116** (2016) 063601.
[37] SAFAVI-NAEINI A. H., GRÖBLACHER S., HILL J. T., CHAN J., ASPELMEYER M. and PAINTER O., *Nature*, **500** (2013) 185.
[38] WOLLMAN E. E., LEI C. U., WEINSTEIN A. J., SUH J., KRONWALD A., MARQUARDT F., CLERK A. A. and SCHWAB K. C., *Science*, **349** (2015) 952.
[39] PALOMAKI T. A., HARLOW J. W., TEUFEL J. D., SIMMONDS R. W. and LEHNERT K. W., *Nature*, **495** (2013) 210.
[40] SHKARIN A. B., FLOWERS-JACOBS N. E., HOCH S. W., KASHKANOVA A. D., DEUTSCH C., REICHEL J. and HARRIS J. G. E., *Phys. Rev. Lett.*, **112** (2014) 013602.
[41] OCKELOEN-KORPPI C. F., DAMSKÄGG E., PIRKKALAINEN J.-M., ASJAD M., CLERK A. A., MASSEL F., WOOLLEY M. J. and SILLANPÄÄ M. A., *Nature*, **556** (2018) 478.
[42] HEINRICH G., LUDWIG M., QIAN J., KUBALA B. and MARQUARDT F., *Phys. Rev. Lett.*, **107** (2011) 043603.
[43] ZHANG M., WIEDERHECKER G. S., MANIPATRUNI S., BARNARD A., MCEUEN P. and LIPSON M., *Phys. Rev. Lett.*, **109** (2012) 233906.
[44] BAGHERI M., POOT M., FAN L., MARQUARDT F. and TANG H. X., *Phys. Rev. Lett.*, **111** (2013) 213902.
[45] TIAN L. and WANG H., *Phys. Rev. A*, **82** (2010) 053806.
[46] SAFAVI-NAEINI A. H. and PAINTER O., *New J. Phys.*, **13** (2011) 013017.
[47] HILL J. T., SAFAVI-NAEINI A. H., CHAN J. and PAINTER O., *Nat. Commun.*, **3** (2012) 1196.
[48] REGAL C. A. and LEHNERT K. W., *J. Phys.: Conf. Ser.*, **264** (2011) 012025.
[49] BOCHMANN J., VAINSENCHER A., AWSCHALOM D. D. and CLELAND A. N., *Nat. Phys.*, **9** (2013) 712.
[50] BAGCI T., SIMONSEN A., SCHMID S., VILLANUEVA L. G., ZEUTHEN E., APPEL J., TAYLOR J. M., SØRENSEN A., USAMI K., SCHLIESSER A. and POLZIK E. S., *Nature*, **507** (2014) 81.
[51] ANDREWS R. W., PETERSON R. W., PURDY T. P., CICAK K., SIMMONDS R. W., REGAL C. A. and LEHNERT K. W., *Nat. Phys.*, **10** (2014) 321.
[52] BALRAM K. C., DAVANÇO M. I., SONG J. D. and SRINIVASAN K., *Nat. Photon.*, **10** (2016) 346.
[53] FORSCH M., STOCKILL R., WALLUCKS A., MARINKOVIC I., GÄRTNER C., NORTE R. A., VAN OTTEN F., FIORE A., SRINIVASAN K. and GRÖBLACHER S., *arXiv:1812.07588*, (2018) .
[54] HAFEZI M. and RABL P., *Opt. Express*, **20** (2012) 7672.
[55] METELMANN A. and CLERK A. A., *Phys. Rev. X*, **5** (2015) 021025.
[56] SHEN Z., ZHANG Y.-L., CHEN Y., ZOU C.-L., XIAO Y.-F., ZOU X.-B., SUN F.-W., GUO G.-C. and DONG C.-H., *Nat. Photon.*, **10** (2016) 657.
[57] RUESINK F., MIRI M.-A., ALÙ A. and VERHAGEN E., *Nat. Commun.*, **7** (2016) 13662.
[58] FANG K., LUO J., METELMANN A., MATHENY M. H., MARQUARDT F., CLERK A. A. and PAINTER O., *Nat. Phys.*, **13** (2017) 465.
[59] BERNIER N. R., TÓTH L. D., KOOTTANDAVIDA A., IOANNOU M. A., MALZ D., NUNNENKAMP A., FEOFANOV A. K. and KIPPENBERG T. J., *Nat. Commun.*, **8** (2017) 604.
[60] PETERSON G. A., LECOCQ F., CICAK K., SIMMONDS R. W., AUMENTADO J. and TEUFEL J. D., *Phys. Rev. X*, **7** (2017) 031001.
[61] BARZANJEH S., WULF M., PERUZZO M., KALAEE M., DIETERLE P. B., PAINTER O. and FINK J. M., *Nat. Commun.*, **8** (2017) 953.

[62] RUESINK F., MATHEW J. P., MIRI M.-A., ALÙ A. and VERHAGEN E., *Nat. Commun.*, **9** (2018) 1798.
[63] SHEN Z., ZHANG Y.-L., CHEN Y., SUN F.-W., ZOU X.-B., GUO G.-C., ZOU C.-L. and DONG C.-H., *Nat. Commun.*, **9** (2018) 1797.
[64] XU H., JIANG L., CLERK A. A. and HARRIS J. G. E., *arXiv:1807.03484*, (2018) .
[65] MATHEW J. P., DEL PINO J. and VERHAGEN E., *arXiv:1812.09369*, (2018) .
[66] SOHN D. B., KIM S. and BAHL G., *Nat. Photon.*, **12** (2018) 91.
[67] KITTLAUS E. A., OTTERSTROM N. T., KHAREL P., GERTLER S. and RAKICH P. T., *Nat. Photon.*, **12** (2018) 613.
[68] PEANO V., BRENDEL C., SCHMIDT M. and MARQUARDT F., *Phys. Rev. X*, **5** (2015) 031011.
[69] SAFAVI-NAEINI A. H., HILL J. T., MEENEHAN S., CHAN J., GRÖBLACHER S. and PAINTER O., *Phys. Rev. Lett.*, **112** (2014) 153603.
[70] THOMPSON J. D., ZWICKL B. M., JAYICH A. M., MARQUARDT F., GIRVIN S. M. and HARRIS J. G. E., *Nature*, **452** (2008) 72.
[71] SANKEY J. C., YANG C., ZWICKL B. M., JAYICH A. M. and HARRIS J. G. E., *Nat. Phys.*, **6** (2010) 707.
[72] LUDWIG M., SAFAVI-NAEINI A. H., PAINTER O. and MARQUARDT F., *Phys. Rev. Lett.*, **109** (2012) 063601.
[73] VANNER M. R., *Phys. Rev. X*, **1** (2011) 021011.
[74] MIAO H., DANILISHIN S., CORBITT T. and CHEN Y., *Phys. Rev. Lett.*, **103** (2009) 100402.
[75] DELLANTONIO L., KYRIIENKO O., MARQUARDT F. and SØRENSEN A. S., *Nat. Commun.*, **9** (2018) 3621.
[76] VANNER M. R., ASPELMEYER M. and KIM M. S., *Phys. Rev. Lett.*, **110** (2013) 010504.
[77] COHEN J. D., MEENEHAN S. M., MACCABE G. S., GRÖBLACHER S., SAFAVI-NAEINI A. H., MARSILI F., SHAW M. D. and PAINTER O., *Nature*, **520** (2015) 522.
[78] GALLAND C., SANGOUARD N., PIRO N., GISIN N. and KIPPENBERG T. J., *Phys. Rev. Lett.*, **112** (2014) 143602.
[79] RIEDINGER R., HONG S., NORTE R. A., SLATER J. A., SHANG J., KRAUSE A. G., ANANT V., ASPELMEYER M. and GRÖBLACHER S., *Nature*, **530** (2016) 313.
[80] RIEDINGER R., WALLUCKS A., MARINKOVIĆ I., LÖSCHNAUER C., ASPELMEYER M., HONG S. and GRÖBLACHER S., *Nature*, **556** (2018) 473.
[81] LEIBFRIED D., BLATT R., MONROE C. and WINELAND D., *Rev. Mod. Phys.*, **75** (2003) 281.
[82] WILSON-RAE I., ZOLLER P. and IMAMOĞLU A., *Phys. Rev. Lett.*, **92** (2004) 075507.
[83] MACQUARRIE E. R., GOSAVI T. A., JUNGWIRTH N. R., BHAVE S. A. and FUCHS G. D., *Phys. Rev. Lett.*, **111** (2013) 227602.
[84] YEO I., DE ASSIS P.-L., GLOPPE A., DUPONT-FERRIER E., VERLOT P., MALIK N. S., DUPUY E., CLAUDON J., GÉRARD J.-M., AUFFÈVES A., NOGUES G., SEIDELIN S., POIZAT J.-P., ARCIZET O. and RICHARD M., *Nat. Nanotech.*, **9** (2014) 106.
[85] OVARTCHAIYAPONG P., LEE K. W., MYERS B. A. and JAYICH A. C. B., *Nat. Commun.*, **5** (2014) 4429.
[86] TEISSIER J., BARFUSS A., APPEL P., NEU E. and MALETINSKY P., *Phys. Rev. Lett.*, **113** (2014) 020503.
[87] ARCIZET O., JACQUES V., SIRIA A., PONCHARAL P., VINCENT P. and SEIDELIN S., *Nat. Phys.*, **7** (2011) 879.
[88] COTRUFO M., FIORE A. and VERHAGEN E., *Phys. Rev. Lett.*, **118** (2017) 133603.
[89] O'CONNELL A. D., HOFHEINZ M., ANSMANN M., BIALCZAK R. C., LENANDER M., LUCERO E., NEELEY M., SANK D., WANG H., WEIDES M., WENNER J., MARTINIS J. M. and CLELAND A. N., *Nature*, **464** (2010) 697.

[90] CHU Y., KHAREL P., RENNINGER W. H., BURKHART L. D., FRUNZIO L., RAKICH P. T. and SCHOELKOPF R. J., *Science*, **358** (2017) 199.

[91] SATZINGER K. J., ZHONG Y. P., CHANG H.-S., PEAIRS G. A., BIENFAIT A., CHOU M.-H., CLELAND A. Y., CONNER C. R., DUMUR E., GREBEL J., GUTIERREZ I., NOVEMBER B. H., POVEY R. G., WHITELEY S. J., AWSCHALOM D. D., SCHUSTER D. I. and CLELAND A. N., *arXiv:1804.07308*, (2018) .

[92] CHU Y., KHAREL P., YOON T., FRUNZIO L., RAKICH P. T. and SCHOELKOPF R. J., *arXiv:1804.07426*, (2018) .